Peer-reviewed version available at J. Compos. Sci. 2019, 3, 61; doi:10.3390/jcs3020061

Article

Effect of silver decoration and light irradiation on the antibacterial activity of TiO_2 and ZnO nanoparticles

Van Thang Nguyen[1], Tien Viet Vu[1], The Huu Nguyen[1],

Tuan Anh Nguyen[2], Thien Vuong Nguyen[2], Phuong Nguyen-Tri[3,4]*

[1] Faculty of Chemical Technology, Hanoi University of Industry, BacTu Liem, Hanoi, Vietnam; email: thangnv2000@me.com

[2]Institute for Tropical Technology, Vietnam Academy of Science and Technology, Hanoi, Vietnam; emails: ntanh2007@gmail.com, vuongvast@gmail.com

[3]Department of Chemistry, University of Montreal, Montreal, Quebec, Canada Phuong.nguyen-tri@umontreal.ca

[4] Département de chimie, biochimie et physique, Université du Québec à Trois-Rivières, Québec, Canada Phuong.Nguyen-Tri@uqtr.ca

* Correspondence: Phuong.nguyen-tri@umontreal.ca; Tel.: +514-340-5121 (ext. 7326)

Received: date; Accepted: date; Published: date

Abstract: This work emphasizes to use silver decorative method to enhance the antibacterial activity of TiO_2 and ZnO nanoparticles. These silver decorated nanoparticles (hybrid nanoparticles) were synthesized by using sodium borohydride as a reducing agent, with the weight ratio of Ag precursors: oxide nanoparticles = 1: 30. The morphology and optical property of these hybrid nanoparticles were investigated using transmission electron microscopy (TEM) and UV–vis spectroscopy. The agar-well diffusion method was used to evaluate their antibacterial activity against both *Staphylococcus aureus* and *Escherichia coli bacteria*, with or without light irradiation. The TEM images indicated clearly that silver nanoparticles (AgNPs, 5-10 nm) were well deposited on the surface of nano-TiO_2 particles (30-60 nm). Besides, smaller AgNPs (< 2 nm) were dispersed on the surface of nano-ZnO particles (20-50 nm). UV-vis spectra confirmed that the hybridization of Ag and oxide nanoparticles led to shift the absorption edge of oxide nanoparticles to the lower energy region (visible region). The antibacterial tests indicated that both oxide pure nanoparticles did not exhibit inhibitory against bacteria, with or without light irradiation. However, the presence of AgNPs in their hybrids, even at low content (< 40 mg/mL) leads to a good antibacterial activity and the higher inhibition zones under light irradiation as compared to that in dark was observed.

Keywords: Silver nanoparticles, nano-TiO_2, nano- ZnO, nanohybrids, antibacterial

1. Introduction

It was reported in literature that nanoparticles can attack bacteria through six main mechanisms [1-15] such as: i) Destruction of the cell wall and peptidoglycan layer; ii) Release of toxic ions; iii) Destruction of protons efflux bombs and modification of membrane charges; iv) Formation of reactive oxygen species (ROS) degrading cell wall; v) Reactive oxygen species (ROS) degrading DNA, RNA and proteins; vi) Low adenosintriphosphat (ATP) production. In case of metallic oxide nanoparticles (such as NiO, Co_3O_4, ZnO, Fe_2O_3, Fe_3O_4, MgO, CuO, TiO_2, SiO_2…), ROS is the predominant antibacterial mechanism, especially for nano-ZnO and Nano-TiO2. For noble metal nanoparticles, such as silver nanoparticles (AgNPs), they can attack effectively against both *Gram-negative* and *Gram-positive* bacteria [16-19], via all 6 mentioned above antimicrobial mechanisms [20-22]. Therefore, in the application AgNPs can be used as the sole antimicrobial agent. AgNPs could also react with bacteria through the photo-catalytic production of ROS in solution [23]. However, Ag^+ free ions released from AgNPs are considered toxic not only to human cells, but also to the environment. Loading (embedding/ immobilizing immobilizing) AgNPs into oxide matrices is new approach due

to its ability to control solubility and toxicity of AgNPs. Various metallic oxide matrices have been used for loading/hybridizing AgNPs, such SiO_2, ZrO_2, Al_2O_3, Fe_3O_4, CuO… [24].

Regarding the metal oxide semiconductor nanoparticles, such as ZnO anh TiO2, they can destroy the pathogenic bacteria by ROS mechanism under UV light radiation. In this case, when a photon of higher energy than their optical band gap energy (Eg~ 3.2-3.4 ev) is absorbed by these nanoparticles, the electron–hole pairs were created and then generated ROS. The practical applications of these nanoparticles are limited due to following two reasons: (i) wide band gap ~3.2 eV for nano-TiO_2 [25]; 3.37 eV for nano-ZnO [26]; and (ii) low photoenergy conversion efficiency [27] with low charge separation efficiency and fast recombination of photogenerated charge carriers) [28, 29]. Two main approachs have been tried to improve the photocatalytic of these nanoparticles: (1) diminution of the recombination for photogenerated electron–hole pairs; and (2) enhancement of the visible light sensitivity [25]. The first pathway focused on the design of heterostructures (heterojunctions), such as (i) deposition of noble metals (Ag, Au or Pt) on the surface of nanoparticles; and (ii) coupling other semiconductor (such as CdSe, Ag_2O, CdS…) with the oxide semiconducting nanoparicles [30-34]. The formation of the Schottky barriers at the interface of noble metals/semiconducting oxide nanoparticles could enhance significantly the segregation of charges, thus reduced the charge recombination [35-36]. In this direction, under UV irradiation, Ubonchonlakate et al. [37] indicated that Ag decorated TiO_2 had higher antibacterial activity (100 % in 10 min) against P.aeruginosa bacteria, than that of pure TiO_2 (57% in 15 min). In other direction, the doping of transition metals/rare earth ions into these oxide crystal lattices could reduce their optical band gap. For TiO_2, the absorption edge was shifted into the lower energy region by S doping [38] and its absorption in visible region increased with the doping content of noble metals [39].

Recently, the hybridization of noble metals (Au, Ag, Pd) and semiconducting oxides becomes the most promising strategy to defeat large band gap of semiconducting oxides [40-44]. The energy level alignment is combined at the heterojunction of these nanoparticles. In the hybrid nanoparticles, the noble metal nanoparticles (gold and silver) exhibit Localized Surface Plasmon resonance (LSPR) absorption in visible light region, which can have significant impact at the heterointerfaces. We published several books and articles on the related topic [21, 40, 45, 64-79].

In this study, the hybridization of AgNPs and ZnO/TiO_2 nanoparticles are expected not only to simply combine property of single components, but also to significantly enhance their antibacterial properties [45]. Thus, this work aims to present the role of silver decoration in enhancing the antibacterial activity of both ZnO and TiO_2 nanoparticles, against two most popular bacteria : *Staphylococcus aureus* (ATCC 25923, Gram-positive) and *Escherichia coli* (Gram-negative, ATCC 25922).

2. Materials and Methods

2.1. Materials

TiO_2 (rutile) and ZnO nanoparticles, were purchased from Sigma Aldrich (Singapore), having a mean diameter <100 nm and a specific surface area of 18 and 15–25 m^2/g, respectively. $AgNO_3$ and $NaBH_4$ were provided by Sigma Aldrich (Thailand).

2.2. Synthesis of silver decorated nanoparticles

0.2 g of TiO_2 (or ZnO) nanoparticles was firstly dispersed in 200 ml of distilled water under ultrasonication. AgNO3 solution (0.01 g in 20 ml water) then slowly added into the prepared nano-TiO_2 (or ZnO) solution under ultrasonication in 30 m. The mixing solution then poured into the 500-ml three-necked pot. Then, $NaBH_4$ solution (0.01 g in 30 ml water) was then added dropwise (1 drop/s) to the 500 ml three-necked pot. The reaction temperature was kept at 4 ºC, and reaction mixture was stirred mechanically for 60 minutes. The nanohybrids were then collected by using centrifugation at 10 000 rpm/min for 5 minutes. The residual precursors and agents were then fully removed after several times of centrifugation by adding fresh distilled water.

2.3. Characterization

The morphologies of the hybrid nanoparticles were investigated using transmission electron microscopy (JEM1010, JEOL, Japan), operating at 80 kV (resolution of 3 Å). UV–Vis spectra were obtained by using a CINTRA 40 spectrophotometer (USA) in absorbance mode with 2 nm slip width.

2.4. Antibacterial tests

The agar-well diffusion method was then used to evaluate their antibacterial activity against Gram-positive (Staphylococcus aureus - ATCC 25923) and Gram-negative (Escherichia coli - ATCC 25922) bacteria. Nutrient agar plates were inoculated in brain heart infusion (BHI) broth using 100 µl of 106 CFU bacterial suspensions. Wells (8 mm diameter) were then punched in the inoculated plates, by using a sterile plastic rod. These wells were then filled with 50 µL of solutions containing nanoparticles, at various concentrations, such as 8, 16 and 40 mg/mL. Control wells were filled with 50 µL of distilled water. These plates were the incubated at 37 ºC for 18 h (with or without light irradiation). After this period, the antibacterial activities of these nanoparticles were evaluated by measuring the inhibition zone diameter around the wells (100 µm resolution; Model: Haloes Caliper - Zone Reader, IUL, Spain).

For light irradiation test, a LED (cold white, 1500 mcd, 3V DC) bulbs (two bulbs) has been used with illumination of ~300 lux. These white LEDs were designed as mixture of blue (450-470 nm) and yellow (560-590 nm) lights that could be perceived by the eye as white color [46].

3. Results and discussions

3.1. Morphological study

Figure 1 shows the electron microscopy images of AgNPs decorated nano-TiO_2 particles. As can be seen in this figure, AgNPs (black particles, 5-10 nm) were well dispersed on the surface of nano-TiO_2 particles (30-60 nm). The bigger nanoparticles are nano-TiO_2 and the smaller ones are AgNPs as well described in the literature [21]. It has to be noted that the synthesis process of hybrid nanoparticles was optimized to obtain the reported sizes of the hybrid nanoparticles.

TEM images of AgNPs decorated nano-ZnO particles are presented in Figure 2. As shown in this figure, small AgNPs (black spots, < 2 nm) were alternatively deposited and linked to nano-ZnO nanoparticles (10-30 nm). These small AgNPs might result in the presence of sharp peak at 410 nm in the UV-vis spectra for these Ag/ZnO nanohybrids (Figure 4 below).

For a comparative study, the size of AgNPs deposited on surface of TiO_2 nanoparticles was higher than that on surface of ZnO nanoparticles.

Peer-reviewed version available at J. Compos. Sci. 2019, 3, 61; doi:10.3390/jcs3020061

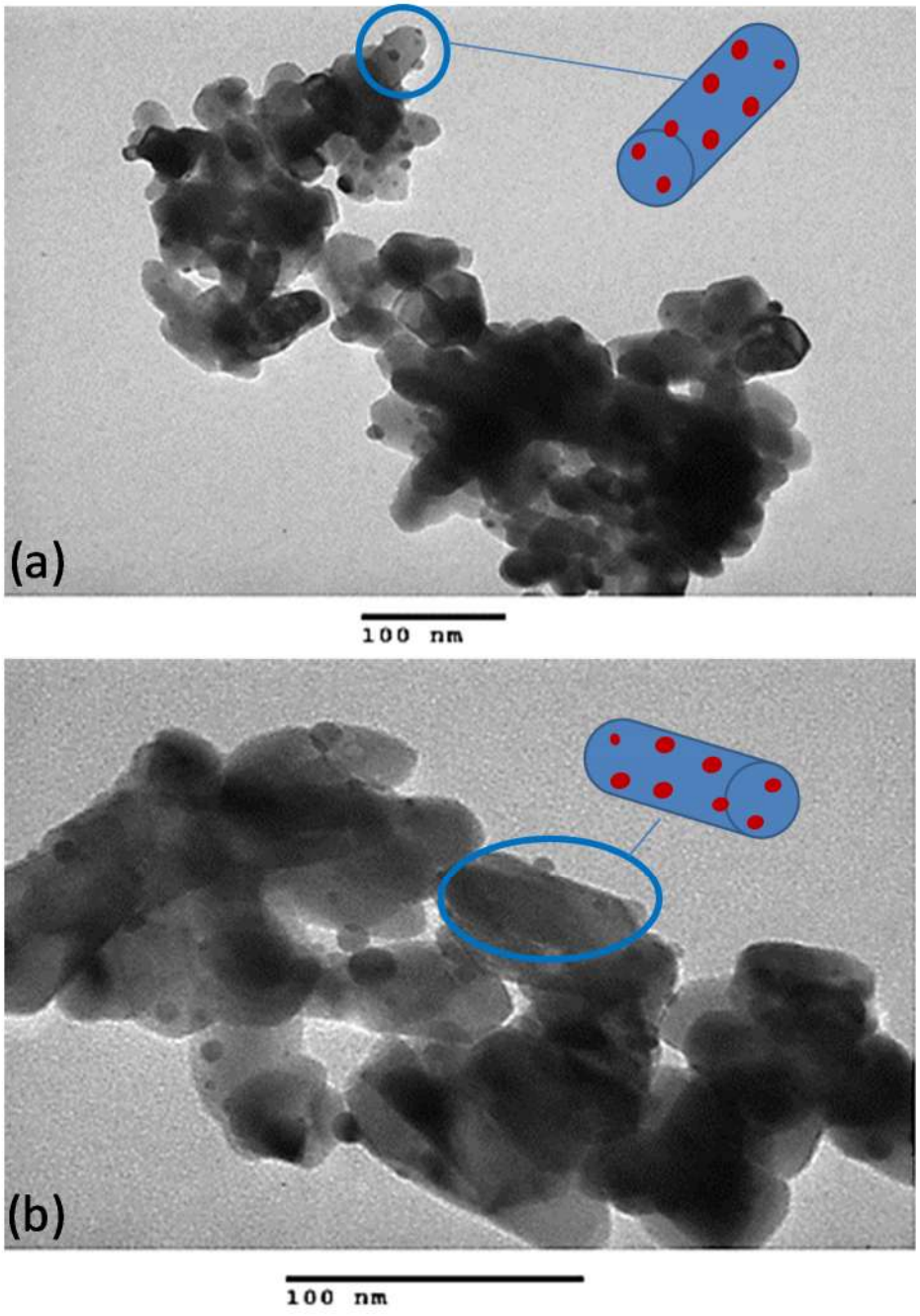

Figure 1. TEM images of Ag loaded TiO_2 nanoparticles at different magnifications showing the hybrid structure; a) 40,000x and b) 80,000x. Inserted images show the schematic illustration of hybrid nanoparticles. Red point represents Ag nanoparticles and bleu support is nano-TiO_2

Peer-reviewed version available at J. Compos. Sci. 2019, 3, 61; doi:10.3390/jcs3020061

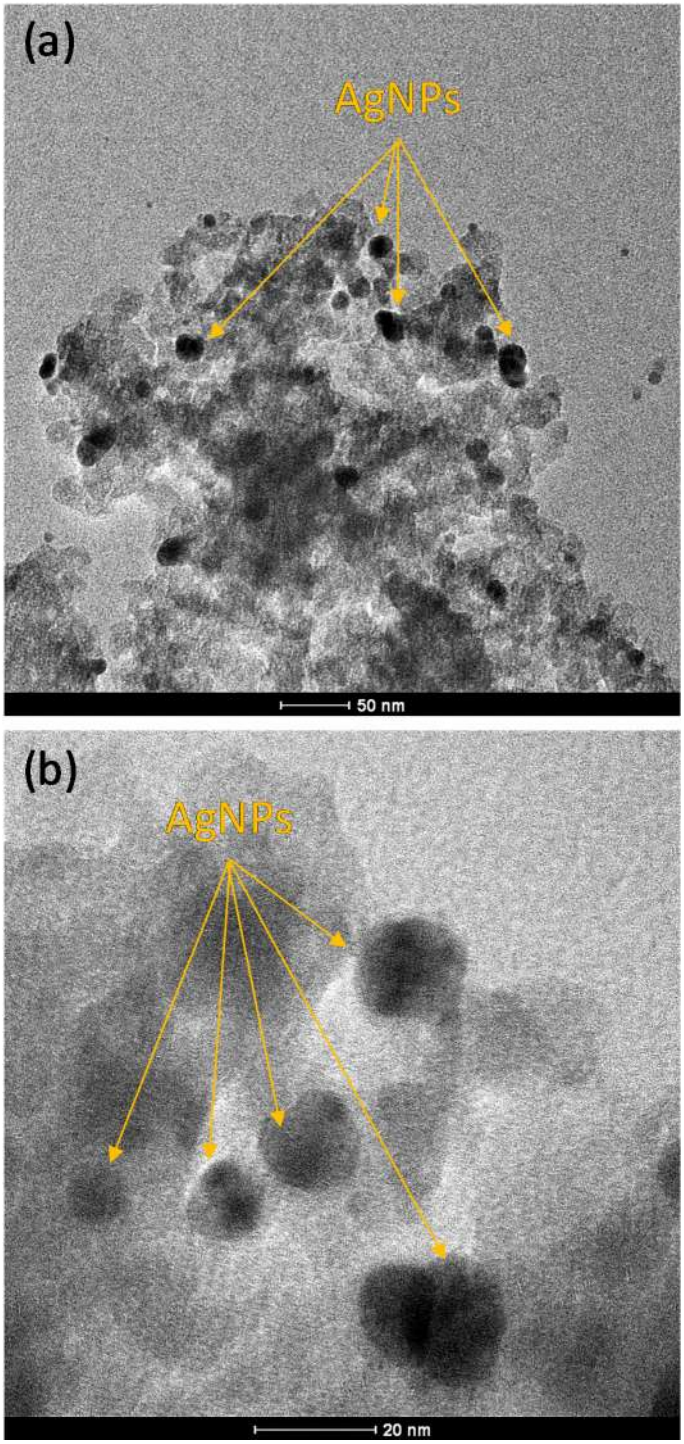

Figure 2. TEM images of Ag loaded ZnO nanoparticles at differenct magnification: a) 30,000x and b) 100,000x.

The UV-visible absorption spectra of AgNPs, nano-TiO_2 and AgNPs decorated nano-TiO_2 particles (dispersed in water) are presented in Figure 3. In case of AgNPs (~10 nm of diameter), broad band around 398 nm was the characteristic of the Surface Plasmon Resonance (SPR peak) of AgNPs [47]. For AgNPs decorated nano-TiO_2 particles, the hybridization of nano-TiO_2 and AgNPs leads to shift the absorption edge to the lower energy region (visible region), as compared with the pure nano-TiO_2 (at 360 nm in the UV region). Similar results were reported for Ag–TiO_2

nanocomposites [48, 49]. The authors signaled that visible light absorption by Surface Plasmon Resonance of AgNPs induced electron transfer to TiO_2, resulting in charge separation and therefore activated by visible light.

Figure 4 shows the UV-visible spectra of AgNPs, nano-ZnO and AgNPs decorated nano-ZnO particles (dispersed in water). As can be seen in Figure 4, a broad band around 410 nm was observed, indicating the presence of AgNPs on the surface of nano-ZnO particles.

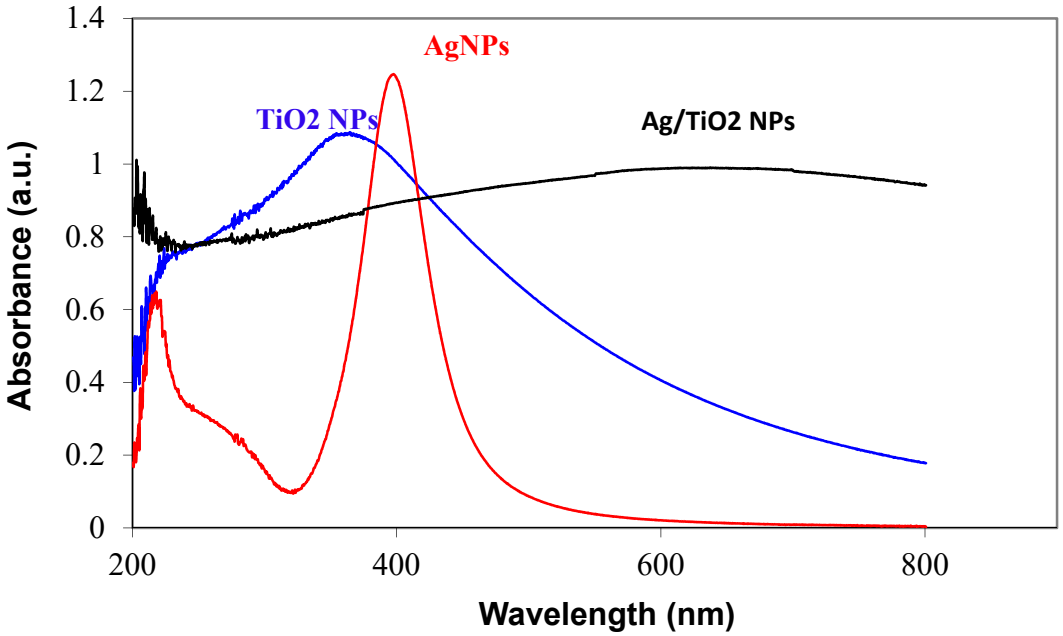

Figure 3. UV-Vis spectra of AgNPs, nano-TiO_2 and AgNPs decorated nano-TiO_2 particles (dispersed in water)

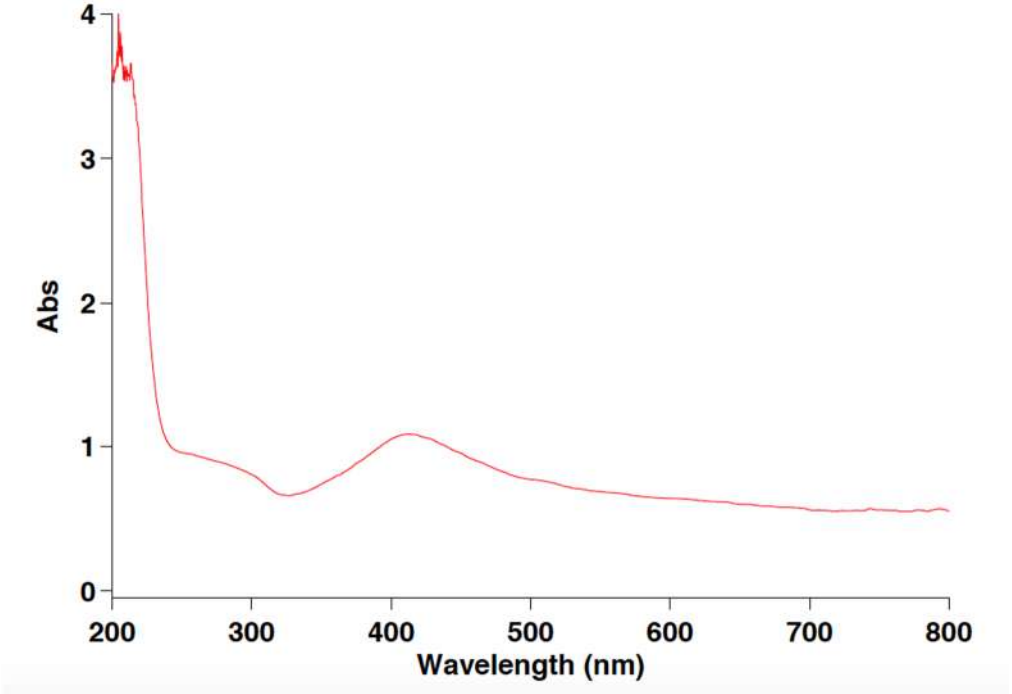

Figure 4. UV-Vis spectra of AgNPs decorated nano-ZnO particles (dispersed in water)

3.2. Antibaterial tests

3.2.1. TiO_2 and Ag/TiO_2 nanoparticles

Figures 5 and 6 present the photographs of antibacterial test for nano-TiO_2 and Ag/TiO_2 NPs against *S. aureus* and *E. coli* bacteria, without and with light irradiation, respectively. Tables 1 and 2 show their corresponding inhibition zones. As shown in Figures 5a and 5b, in the dark TiO_2 NPs did not exhibit inhibitory effects on *S. aureus* bacteria (at concentrations of 10-40 mg/mL), whereas Ag loaded TiO_2 NPs exhibited significant antibacterial activity at the concentration of 40 mg/mL). It was reported that TiO_2 nanoparticles are easy to attach to the cell membranes and accumulate [50]. In general, TiO_2 nanoparticles can destroy the pathogenic bacteria by ROS mechanism under UV light radiation. Since the emitted wavelengths of the white LED lights include peaks in the blue (450-470 nm) and yellow (560-590nm) areas, the inhibition zone of Ag loaded TiO_2 NPs (40 mg/mL) could be attributed to the content of AgNPs in the nanohybrids (e.g ~1.3 mg/mL). Please note that the concentration of TiO_2 in nanohybrids is 30 times higher than that of AgNPs (from synthesis: the weight ratio of Ag precursors: TiO_2 = 1: 30). Besides, Ubonchonlakate et al. [51] reported that Ag doped TiO_2 had higher antibacterial efficiency (100 % in 10 min) against *P. Aeruginosa* bacteria than that of pure TiO_2 (57% in 15 min), under UV irradiation. The interesting results are observed under light irradiation for Ag/TiO_2 nanohybrids (Table 1). These nanoparticles exhibited the inhibition zone of 2 mm (in diameter) at the lower concentration of 16 mg/mL, indicating the contribution of TiO_2 nanoparticles in this nanohybrids to their antibacterial activity. At the high concentration of 40 mg/mL, their inhibition zone is similar to the case in dark (4 mm in diameter), indicating the dominated contribution of AgNPs to the antibacterial activity of these nanohybrids (at this high concentration).

As seen in Figures 5c and 5d, TiO_2 NPs did not exhibit inhibitory effects under this light irradiation on these bacteria (at concentration of 8-40 mg/mL). It was reported that the absorption of light in the visible region of TiO_2 increased with the noble metals (Pt, Au and Pd) doping content [52]. Yue Lin et al. [53] also reported the antibacterial properties against *E.coli* of the Ag/TiO_2 core/shell nanoparticles without the presence of UV light. They observed the obvious zone of inhibition around the hybrid nanoparticles, whereas there was no inhibition detected around the pure TiO_2 nanoparticles. Similar results also were observed by Dhanalekshmi et al [54] for Ag/TiO_2 core/shell hybrid nanoparticles against *E.coli* and *S.aureus* bacteria. Zhang et al. [55] reported TiO_2 nanoparticles with highly dispersed Ag clusters are entirely restricted the *E. coli* bacterial growth [55]. Barudin et al. [56] indicated that Ag-TiO_2 nanoparticles exhibited the superior antibacterial activity, as compared to the lone individual TiO_2 nanoparticles, under visible light irradiation [56].

In this work, for *E.coli* bacteria, under light irradiation Ag/TiO_2 nanohybrids have the higher antibacterial activity than that in darkness (Table 2, with concentration of 8 and 16 mg/mL), due to the hybridization of AgNPs and TiO_2 NPs. Besides, in dark, the inhibition zones of Ag/TiO_2 nanohybrids increase with their concentration, due to the increase of AgNPs in the nanohybrids.

Preprints (www.preprints.org) | NOT PEER-REVIEWED | Posted: 24 May 2019 doi:10.20944/preprints201905.0298.v1

Peer-reviewed version available at J. Compos. Sci. 2019, 3, 61; doi:10.3390/jcs3020061

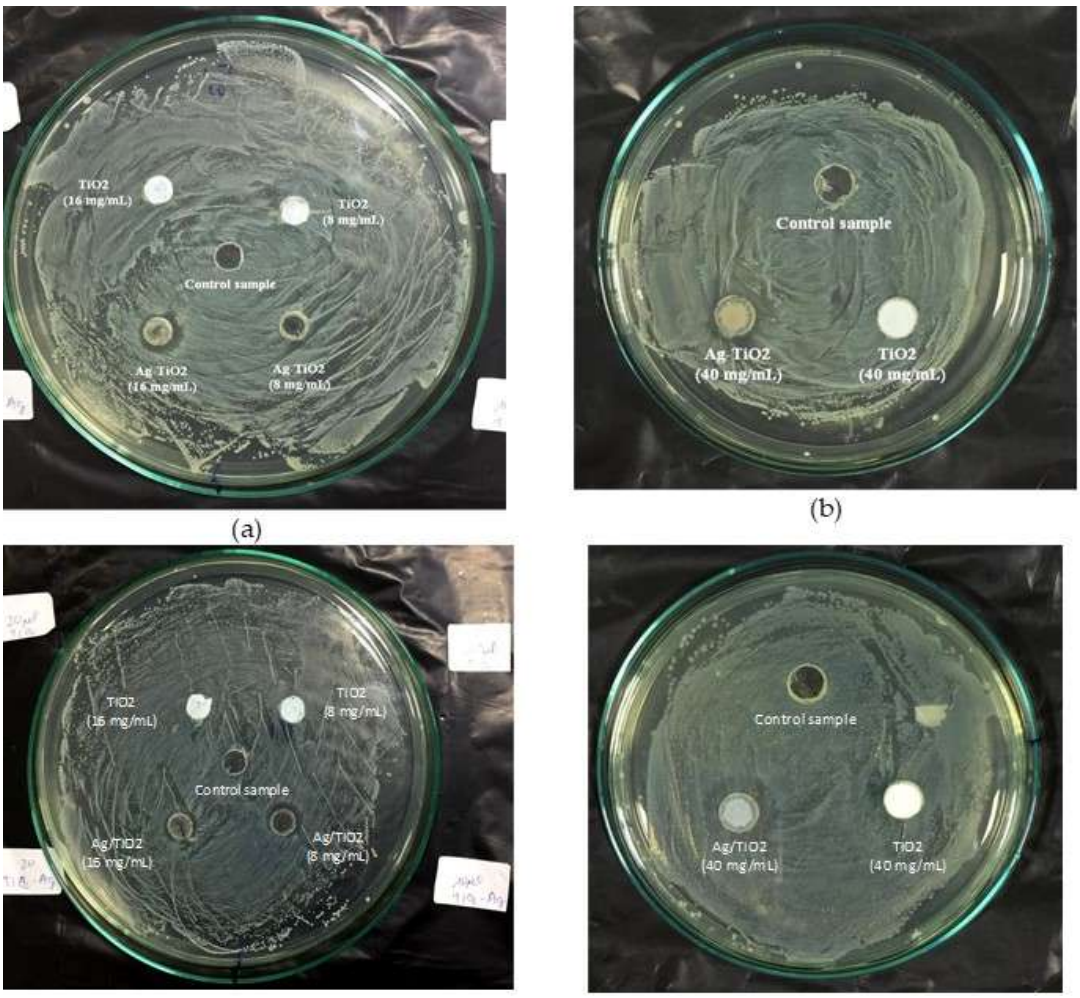

202

203 **Figure 5.** Photographs of antibacterial test against *S. aureus* bacteria (agar-well diffusion
204 method) for pure TiO_2 and Ag loaded TiO_2 nanoparticles (a and b: without light irradiation; c and d:
205 without light irradiation). Concentrations of 8, 16 and 40 mg/mL.

206

Figure 6. Photographs of antibacterial test against *E. coli* bacteria (agar-well diffusion method) for Ag loaded TiO_2 nanoparticles: a) without light irradiation; b) under light irradiation). Concentration of 8, 16 and 40 mg/mL.

Table 1: Antibacterial activity against *S. aureus* bacteria of TiO_2 nanoparticles and Ag loaded TiO_2 nanoparticles

Concentrations (mg/mL)	**Inhibition Zone (mm)**			
	without light irradiation		**under light irradiation**	
	TiO_2 nanoparticles	Ag decorated TiO_2 nanoparticles	TiO_2 nanoparticles	Ag decorated TiO_2 nanoparticles
8	0	0	0	0
16	0	0	0	2
40	0	4	0	4

Table 2: Antibacterial activity against *E. coli* bacteria of TiO_2 nanoparticles and Ag loaded TiO_2 nanoparticles

Concentrations (mg/mL)	**Inhibition Zone (mm)**			
	without light irradiation		**under light irradiation**	
	TiO_2 nanoparticles	Ag decorated TiO_2 nanoparticles	TiO_2 nanoparticles	Ag decorated TiO_2 nanoparticles
8	0	2	0	6
16	0	6	0	8
40	0	8	0	8

3.2.2. ZnO and Ag/ZnO nanoparticles

It was reported in literature that ZnO has the inherent gain of broad antibacterial activities against virus, bacteria, fungus and spores [57-59]. Stoimenov et al. [60] defined that ZnO nanoparticles attached on the bacterial surface due to electrostatic force of attraction. We expect that the hybridization of AgNPs with ZnO NPs may exhibit the superior antibacterial activity, as compared to the lone individual NPs [45].

Figures 7 and 8 show the photographs of antibacterial test for nano-ZnO and Ag/ZnO NPs against *S. aureus* and *E. coli* bacteria, without and with light irradiation, respectively. Tables 3 and 4 show their corresponding inhibition zones. As shown in Figures 7 and 8, ZnO NPs did not exhibit inhibitory effects on both bacteria with or without light irradiation (at concentrations of 10-40 mg/mL).

For Ag/ZnO nanohybrids, as shown in Tables 3 and 4, light irradiation increases the diameter of inhibition zone for both *S. aureus* (at 8 mg/mL) and *E. coli* (at 8, 16, 40 mg/mL) bacteria. Similarity, Mariana Ibanescu et al. [61] reported the antimicrobial property of Ag/ZnO nanocomposites against both *E. coli* and *M. luteus* bacteria. The authors found that small amounts of silver could significantly enhance the antimicrobial activity. The photocatalytic activity of Ag/ZnO nanocomposites could contribute to their high antimicrobial activity. Nagaraju et al. [62] also indicated the high

antimicrobial activity of Ag-ZnO NPs against both *E. coli* and *S. aureus* bacteria. The inhibition zone could be observed at the concentration of 500 μg Ag-ZnO NPs. Wei et al. [63] also described the high antibacterial activity of Ag-ZnO hybrid nanofibres against *E. coli* and *P. aeruginosa* bacteria.

For the comparative study, under light irradiation at the low concentration (8 mg/mL), Ag/ZnO nanohybrids exhibit the higher antibacterial activity against both two bacteria, than Ag-Ag/TiO_2 nanohybrids. One possible explanation is the better homogeneous deposition of the smaller AgNPs on the surface of nano-ZnO particles, as compared to that of nano-TiO_2 nanoparticles (Figures 1 and 2).

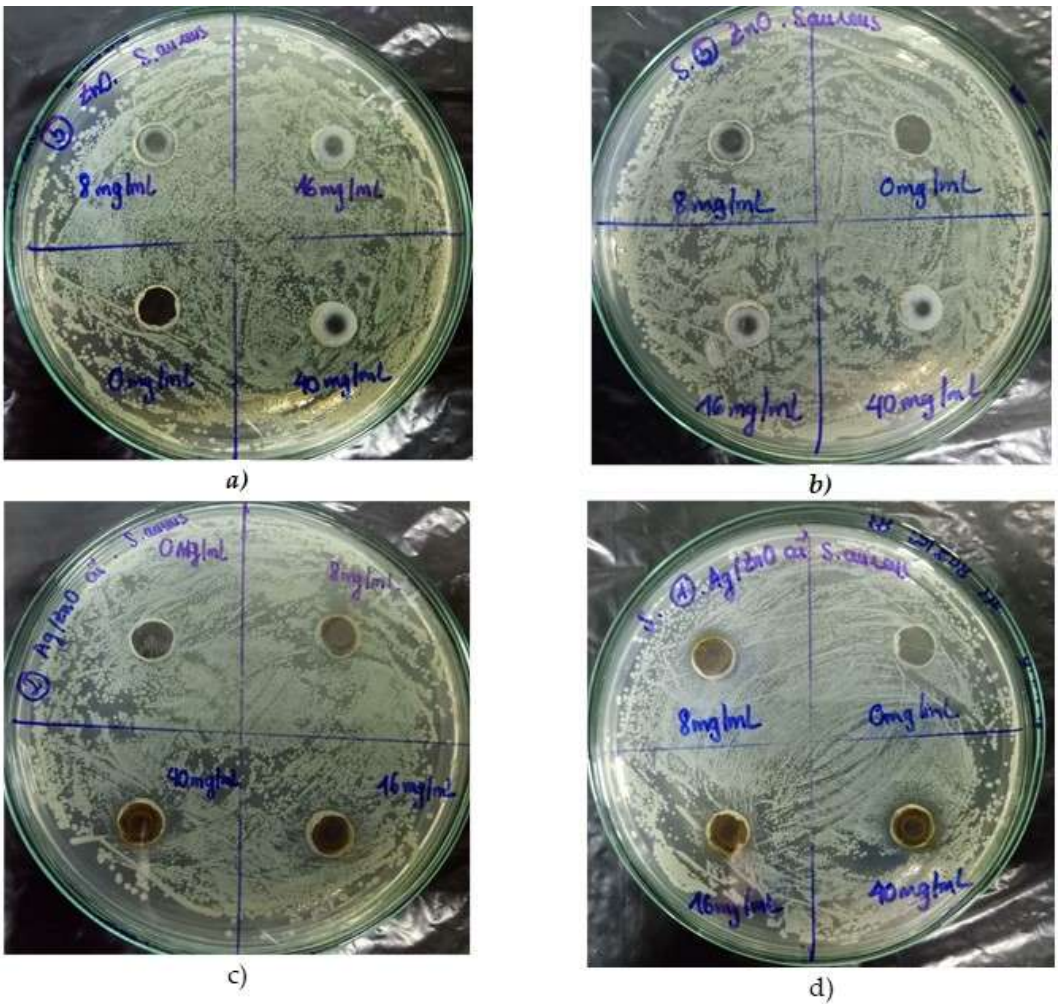

Figure 7. Photographs of antibacterial test against *S. aureus* bacteria (agar-well diffusion method) for pure ZnO nanoparticles (a: without light irradiation; b: under light irradiation) and Ag loaded ZnO nanoparticles (c: without light irradiation; d: under light irradiation). Concentration of 8, 16 and 40 mg/mL.

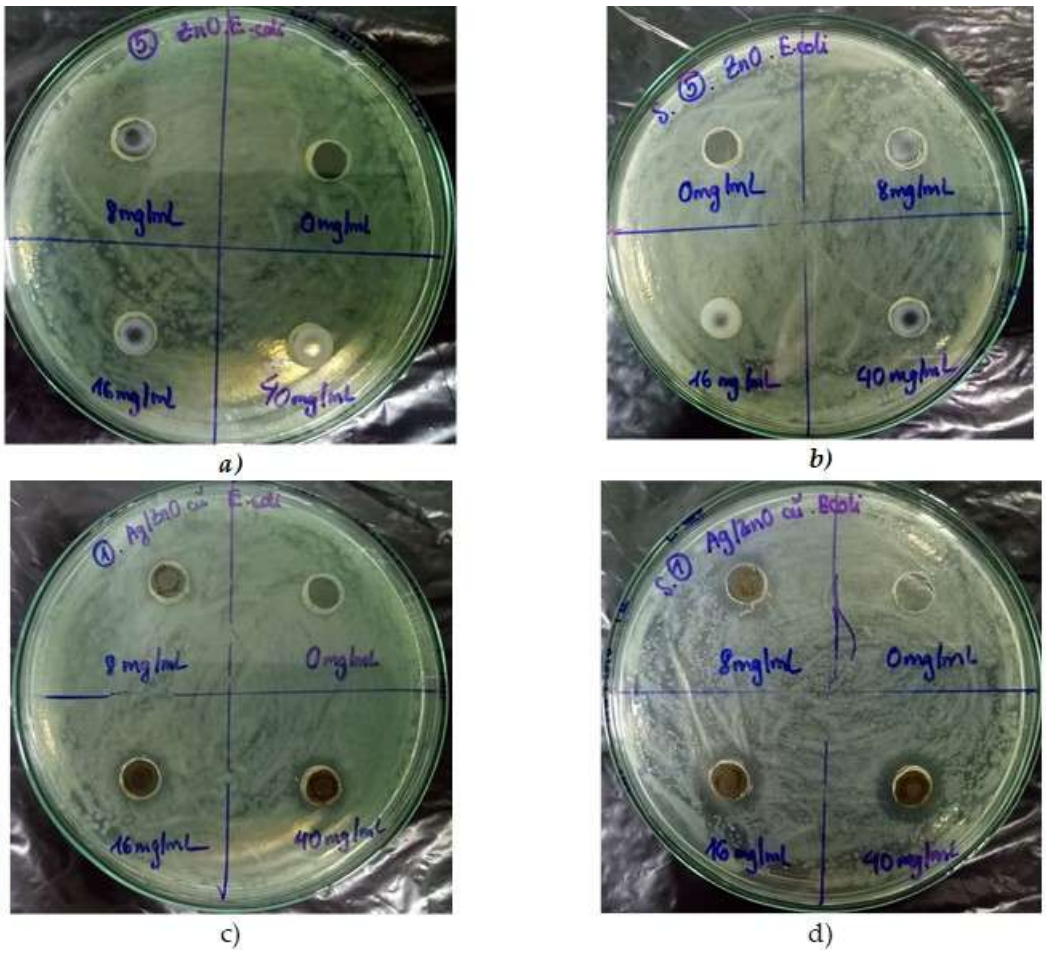

Figure 8. Photographs of antibacterial test against *E. coli* bacteria (agar-well diffusion method) for ZnO nanoparticles (a-without light irradiation; b-under light irradiation) and and Ag loaded ZnO nanoparticles (c-without light irradiation; d-under light irradiation). Concentration of 8, 16 and 40 mg/mL.

Table 3: Antibacterial activity against *S. aureus* bacteria of ZnO nanoparticles and Ag loaded ZnO nanoparticles

Concentrations (mg/mL)	Inhibition Zone (mm)			
	without light irradiation		under light irradiation	
	ZnO nanoparticles	Ag decorated ZnO nanoparticles	ZnO nanoparticles	Ag decorated ZnO nanoparticles
8	0	0	0	2
16	0	2	0	2
40	0	4	0	4

Table 4: Antibacterial activity against *E. coli* bacteria of ZnO nanoparticles and Ag loaded ZnO nanoparticles

Concentrations (mg/mL)	Inhibition Zone (mm)			
	without light irradiation		under light irradiation	
	ZnO nanoparticles	Ag decorated ZnO nanoparticles	ZnO nanoparticles	Ag decorated ZnO nanoparticles
8	0	2	0	7
16	0	4	0	8
40	0	6	0	8

4. Conclusions

The main findings of this work were as follows:

1. Silver decorated oxide nanoparticles have been successfully synthesized by using sodium borohydride as reducing agent, with the weight ratio of Ag precursors: oxide nanoparticles = 1: 30.
2. The TEM images indicated that AgNPs (5-10 nm) were deposited on the surface of nano-TiO2 particles (30-60 nm). Whereas, the smaller AgNPs (< 2 nm) were dispersed on the surface of nano-ZnO particles (10-30 nm).
3. UV-vis spectra indicated that the hybridization of Ag and oxide nanoparticles led to shift the absorption edge of oxide nanoparticles to the lower energy region (visible region).
4. The antibacterial tests indicated that both oxide nanoparticles did not exhibit inhibitory against bacteria, with or without light irradiation. However, the presence of AgNPs in their hybrids (at the concentration < 40 mg/mL) exhibited the higher inhibition zones under light irradiation, as compared to that in dark. At the high concentration of 40 mg/mL, the antibacterial behavior of these nanohybrids under light irradiation is similar to that in dark, indicating the dominated contribution of AgNPs to the antibacterial activity of these nanohybrids (at this high concentration).
5. As the comparative study, under light irradiation at the low concentration (8 mg/mL), Ag/ZnO nanohybrids exhibit the higher antibacterial activity against both two bacteria, than the Ag-Ag/TiO_2 nanohybrids.

Author Contributions: Conceptualization and methodology, N.T.P.; N.T.A; synthesis of ZnO-AgNPs: T.V.V and N.T.V; Synthesis of TiO_2-AgNPs: T.H.N; writing—original draft preparation, N.T.A; writing—review and editing N.T.P.; supervision, N.T.P.;

Funding: This work was financial supported by Natural Sciences and Engineering Research Council of Canada (NSERC).

Conflicts of Interest: The authors declare no conflict of interest.

References

1. Rai VR, Bai AJ., Nanoparticles and their potential application as antimicrobials. In: Science against microbial pathogens: Communicating current research and technological advances, Méndez-Vilas A. Ed., Formatex, Microbiology Series No.3, Vol.1, Badajoz, Spain. 97-209, 2011.
2. BECON Nanoscience and Nanotechnology Symposium Report, National Institutes of Health Bioengineering Consortium, National Institute of Health, USA, 2000. http://www.uta.edu/rfmems/060515-NSF-NUE/Info/biomed/nanotechsympreport.pdf

3. Q. Li, S Mahendra, D Y Lyon, L Brunet, MV Liga, D Li, P J J Alvarez, Antimicrobial nanomaterials for water disinfection and microbial control: Potential applications and implications. Water Res., 42 (2008) 4591–4602
4. E. Oesterling, N Chopra, V Gavalas, X Arzuaga, E J Lim, R Sultanab, D A Butterfield, L Bachas, B Hennig, Alumina nanoparticles induce expression of endothelial cell adhesion molecules. Toxicol Lett., 178 (2008) 160-166.
5. S. Dey, V. Bakthavatchalu, M. T . Tseng, P. Wu, R. L. Florence, E. A. Grulke, R. A. Yokel, S. K. Dhar, H. S. Yang, Y. Chen, D. K. St Clair, Interactions between SIRT1 and AP-1 reveal a mechanistic insight into the growth promoting properties of alumina (Al2O3) nanoparticles in mouse skin epithelial cells, Carcinogenesis, 29 (2008) 1920–1929.
6. Y. N. Chang, M Zhang, L Xia, J Zhang, G Xing, The Toxic Effects and Mechanisms of CuO and ZnO Nanoparticles, Materials, 5 (2012) 2850-2871.
7. H. L. Karlsson, P Cronholm, J Gustafsson, L Moller, Copper oxide nanoparticles are highly toxic: A comparison between metal oxide nanoparticles and carbon nanotubes, Chem Res Toxicol. 21 (2008)1726–1732.
8. T. Xia, M. Kovochich, M. Liong, L. Mädler, B. Gilbert, H. Shi, J. I. Yeh, J. I. Zink, A. E. Nel, Comparison of the mechanism of toxicity of zinc oxide and cerium oxide nanoparticles based on dissolution and oxidative stress properties, ACS Nano. 23 (2008) 2121-2134.
9. S. M. Hussain, K. L. Hess, J. M. Gearhart, K. T. Geiss, J. J. Schlager, In vitro toxicity of nanoparticles in BRL 3A rat liver cells, Toxicol In Vitro. 19 (2005) 975–983.
10. G Ren, D Hu, EW Cheng, MA Vargas-Reus, P Reip, RP Allaker, Characterisation of copper oxide nanoparticles for antimicrobial applications. J Antimicrob Agents., 33(2009) 587-90.
11. J Niskanen, J Shan, H Tenhu, H Jiang, E Kauppinen, V Barranco, F Pico, K Yliniemi, K. Kontturi, Synthesis of copolymerstabilized silver nanoparticles for coating materials. Colloid Polym Sci. 288 (2010) 543–553.
12. J P Guggenbichler, M Böswald, S Lugauer, T Krall, A new technology of microdispersed silver in polyurethane induces antimicrobial activity in central venous catheters, Infection, 27 Suppl 1 (1999) S16-23.
13. A Azam, AS Ahmed, M Oves, MS Khan, A. Memic, Size-dependent antimicrobial properties of CuO nanoparticles against Gram-positive and -negative bacterial strains Int J Nanomedicine, 7 (2012) 3527–3535.
14. RP. Allaker, The use of nanoparticles to control oral biofilm formation, J dent Res. 89 (2010) 1175-1185.
15. C. L. Santos, A. J. R. Albuquerque, F. C. Sampaio and D. Keyson, Nanomaterials with Antimicrobial Properties: Applications in Health Sciences, In: Microbial pathogens and strategies for combating them: Science, Technology and Education, A. Méndez-Vilas Ed., Formatex, 2013, Badajoz, Spain.
16. H. H. Huang, X. P. Ni, G. L. Loy, C. H. Chew, K. L. Tan, F. C. Loh, J. F. Deng, and G. Q. Xu, Photochemical Formation of Silver Nanoparticles in Poly(N-vinylpyrrolidone), Langmuir 12 (1996) 909-912. DOI: 10.1021/la950435d
17. E. Weir, A. Lawlor, A. Whelan, and F. Regan, The use of nanoparticles in anti-microbial materials and their characterization, Analyst 133 (2008) 835-845. doi: 10.1039/b715532h.
18. C M Jones, E M V Hoek, A review of the antibacterial effects of silver nanomaterials and potential implications for human health and the environment, J. Nanopart. Res. 12 (5) (2010) 1531-1551.
19. M.A. Shenashen, S.A. El-Safty, E.A. Elshehy, Synthesis, morphological control, and properties of silver nanoparticles in potential applications, Part. Part. Syst. Charact. 31 (2014) 293–316, doi:10.1002/ppsc.201300181.
20. Q Li, S Mahendra, DY Lyon, L Brunet, MV Liga, D Li, PJJ Alvarez, Antimicrobial nanomaterials for water disinfection and microbial control: Potential applications and implications, Water Res. 42 (2008) 4591–4602
21. P. Nguyen-Tri, V. T. Nguyen, T. A. Nguyen, Biological activity and nanostructuration of Fe_3O_4-Ag /polyethyelene nanocomposites, Journal of Composites Science, 2019, 3 (2) https://doi.org/10.3390/jcs474493
22. SM Hussain, KL Hess, JM Gearhart, KT Geiss, JJ Schlager, In vitro toxicity of nanoparticles in BRL 3A rat liver cells, Toxicol In Vitro. 19(2005) 975–983.
23. B. Le Ouay, F. Stellacci, Antibacterial activity of silver nanoparticles: a surface science insight, Nano Today 10 (2015) 339–354, doi:10.1016/j.nantod.2015.04.002.
24. K. I. Dhanalekshmi, Van Thang Nguyen, P. Magesan, Chapter 26: Nanosilver loaded oxide nanoparticles for antibacterial application, In: "Smart nanocontainers: Fundamentals and Emerging Applications", Eds: Phuong Nguyen-Tri, Trong-On Do, Tuan Anh Nguyen, (2019) Elsevier. ISBN: 9780128167700

25. O. Akhavan, Lasting antibacterial activities of Ag-TiO_2/Ag/a-TiO_2 nanocomposite thin film photocatalysts under solar light irradiation, Journal of Colloid and Interface Science, 336 (1) 2009 117-124. https://doi.org/10.1016/j.jcis.2009.03.018
26. H. Gholap, S. Warule, J. Sangshetti, G. Kulkarni, A. Banpurkar, S. Satpute, R. Patil, Hierarchical nanostructures of Au@ZnO: antibacterial and antibiofilm agent, Appl Microbiol Biotechnol, 100 (13) (2016) 5849-5858. doi: 10.1007/s00253-016-7391-1
27. Y Tamaki, K Hara, R Katoh, M Tachiya, A Furub Femtosecond visible-to-IR spectroscopy of TiO2 nanocrystalline films: elucidation of the electron mobility before deep trapping. J Phys Chem C, 113 (2009) 11741–11746
28. X. Chen, S.S. Mao, Titanium dioxide nanomaterials: synthesis, properties, modifications and applications, Chem. Rev. 107 (2007) 2891-2959.
29. A. Kudo, Y. Miseki, Heterogeneous photocatalyst materials for water splitting, Chem. Soc. Rev. 38 (2009) 253-278
30. L. Sun, J. Li, C. Wang, S. Li, Y. Lai, H. Chen, C. Lin, Ultrasound aided photochemical synthesis of Ag loaded TiO2 nanotube arrays to enhance photocatalytic activity, J. Hazard. Mater. 171 (2009) 1045-1050.
31. Md. A. A. Mamun, Y. Kusumoto, T. Zannat, S. Md Islam, Synergistic enhanced photocatalytic and photothermal activity of Au@TiO2 nanopellets against human epithelial carcinoma cells, Phys. Chem. Chem. Phys. 13 (2011) 21026-21034.
32. J.S. Jang, S.H. Choi, H.G. Kim, J.S. Lee, Location and state of Pt in platinized CdS/TiO2 photocatalysts for hydrogen production from water under visible light, J. Phys. Chem. C 112 (2008) 17200-17205.
33. D. Sarkart, C.K. Ghosh, S. Mukherjee, K.K. Chattopadhyay, Three dimensional Ag2O/TiO2 type-II (p-n) nanoheterojunctions for superior photocatalytic activity, ACS Appl. Mater. Interfaces 5 (2013) 331-337.
34. Y.F. Ji, W. Guo, H.H. Chen, L.S. Zhang, S. Chen, M.T. Hua, Y.H. Long, Z. Chen Surface Ti3+/Ti4+ redox shuttle enhancing photocatalytic H2 production in ultrathin TiO2 nanosheets/CdSe quantum dots, J. Phys. Chem. C 119 (2015) 27053-7059.
35. Q. Deng, H.B. Tang, G. Liu, X.P. Song, G.P. Xu, Q. Li, D.H.L. Ng, G.Z. Wang, The fabrication and photocatalytic performances of flower-like Ag nanoparticles/ZnO nanosheets-assembled microspheres, Appl. Surf. Sci. 331(2015) 50–57.
36. Y.M. Liang, N. Guo, L.L. Li, R.Q. Li, G.J. Ji, S.C. Gan, Fabrication of porous 3D flower-like Ag/ZnO heterostructurecomposites with enhanced photocatalytic performance, Appl. Surf. Sci. 332 (2015) 32–39.
37. K. Ubonchonlakate, L. Sikong, F. Saito, Photocatalytic disinfection of P.aeruginosa bacterial Ag-doped TiO2 film, Procedia Eng. 32 (2012) 656–662.
38. T. Umebayashi, T. Yamaki, S. Tanaka, K. Asai, Visible light-induced degradation of methylene blue on S-doped TiO2, Chem. Lett. 32 (2003) 330–331.
39. S. Sakthivel, M.V. Shankar, M. Palanichamy, B. Arabindoo, D.W. Bahnemann, V.Murugesan, Enhancement of photocatalytic activity by metal deposition:characterisation and photonic efficiency of Pt, Au and Pd deposited on TiO2 catalyst, Water Res. 38 (2004) 3001–3008.
40. Mohapatra, S.; Nguyen, T.A.; Nguyen-Tri, P. Noble Metal-Metal Oxide Hybrid Nanoparticles: Fundamentals and Applications; Elsevier: Amsterdam, The Netherlands, 2018; Volume 1.
41. Fageria, P., Gangopadhyay, S. & Pande, S. Synthesis of ZnO/Au and ZnO/Ag nanoparticles and their photocatalytic application using UV and visible light. RSC Adv.4, 24962-24972, doi:10.1039/c4ra03158j (2014).
42. Xu, C. et al. Fabrication of visible-light-driven Ag/TiO2 heterojunction composites induced by shock wave. Journal of Alloys and Compounds679, 463-469, doi:10.1016/j.jallcom.2016.04.048 (2016).
43. Xu, F. et al. Au nanoparticles modified branched TiO2 nanorod array arranged with ultrathin nanorods for enhanced photoelectrochemical water splitting. Journal of Alloys and Compounds693, 1124-1132, doi:10.1016/j.jallcom.2016.09.273 (2017).
44. Chang, Y. et al. Optical Properties and Photocatalytic Performances of Pd Modified ZnO Samples. The Journal of Physical Chemistry C113, 18761-18767, doi:10.1021/jp9050808 (2009).
45. Phuong Nguyen Tri, Tuan Anh Nguyen, The Huu Nguyen, Pascal Carriere, Antibacterial Behavior of Hybrid Nanoparticles (Chapter 7), In: "Noble Metal-Metal Oxide Hybrid Nanoparticles: Fundamentals and Applications", Eds: Satyabrata Mohapatra, Tuan Anh Nguyen, Phuong Nguyen-Tri (2019) 141-155. Elsevier, https://doi.org/10.1016/B978-0-12-814134-2.00007-3

46. Standard and White LED Basics and Operation, https://www.maximintegrated.com/en/app-notes/index.mvp/id/3070
47. Kuriakose, S., Choudhary, V., Satpati, B. & Mohapatra, S. Enhanced photocatalytic activity of Ag-ZnO hybrid plasmonic nanostructures prepared by a facile wet chemical method. Beilstein J Nanotechnol5, 639-650, doi:10.3762/bjnano.5.75 (2014).
48. M. K. Seery, R. George, P. Floris, S.C. Pillai, Silver doped titanium dioxide nanomaterials for enhanced visible light photocatalysis, J. Photochem. Photobiol. A, 189 (2-3) (2007) 258-263. https://doi.org/10.1016/j.jphotochem.2007.02.010
49. Y. Tian, T. Tatsuma, Plasmon-induced photoelectrochemistry at metal nanoparticles supported on nanoporous TiO2, Chem. Commun. 16 (2004) 1810-1811. DOI: 10.1039/B405061D
50. R. Cai, K. Hashimoto, K. Itoh, Y. Kubota, A. Fujishima, Photokilling of Malignant cells with ultrafine TiO2 powders, Bull.Chem. Soc. 64 (1991) 1268-1273
51. K. Ubonchonlakate, L. Sikong, F. Saito, Photocatalytic disinfection of P.aeruginosa bacterial Ag-doped TiO2 film, Procedia Eng. 32 (2012) 656–662.
52. S. Sakthivel, M.V. Shankar, M. Palanichamy, B. Arabindoo, D.W. Bahnemann, V.Murugesan, Enhancement of photocatalytic activity by metal deposition:characterisation and photonic efficiency of Pt, Au and Pd deposited on TiO2 catalyst, Water Res. 38 (2004) 3001–3008
53. L. Yue, Q. Wang, X. Zhang, Z. Wang, W. Xia, Y. Dong, Synthesis of Ag/TiO_2 Core/Shell Nanoparticles with Antibacterial Properties, Bull. Korean Chem. Soc., 32 (8) (2011) 2607-2610. DOI : 10.5012/bkcs.2011.32.8.2607
54. K. I. Dhanalekshmi, K. S. Meen, I. Ramesh, Synthesis and Characterization of Ag@TiO_2 Core-shell nanoparticles and study of its antibacterial activity, International Journal of Nanotechnology and Application, 3 (5) (2013) 5-14
55. H. Zhang, G. Chen, Potent Antibacterial Activities of Ag/TiO2 Nanocomposite Powders Synthesized by a One-Pot Sol−Gel Method, Environ. Sci. Technol. 43 (8) (2009) 2905–2910
56. Nur Hidayati Ahmad Barudin, Srimala Sreekantan, Ong Ming Thong, Geethaa Sahgal, Antibacterial Activity of Ag-TiO2 Nanoparticles with Various Silver Contents Materials Science Forum Vol. 756 (2013) 238-245.
57. T Jin, D Sun, JY Su, H Zhang, HJ Sue, Antimicrobial Efficacy of Zinc Oxide Quantum Dots against Listeria monocytogenes, Salmonella Enteritidis, and Escherichia coli O157:H7. 74(1) (2009) M46–M52
58. K. M. Kumar, B. K. Mandal, E. A.Naidu, M. Sinha, K. S. Kumar, P. S. Reddy, Synthesis and Characterization of Flower Shaped Zinc Oxide Nanostructures and Its Antimicrobial Activity. Spectrochim. Acta, Part A, 104 (2013) 171−174.
59. A. Lipovsky, Y. Nitzan, A. Gedanken, R. Lubart, Antifungal Activity of ZnO Nanoparticles - the Role of ROS Mediated Cell Injury. Nanotechnology, 22 (2011) 105101.
60. P K Stoimenov, R L Klinger, G L Marchin, K J Klabunde, Metal oxide nanoparticles as bactericidal agents. Langmuir 18 (2002) 6679–6686
61. Mariana Ibanescu, Viorica Muşat, Torsten Textor, Viorel Badilita Boris Mahltig, Photocatalytic and antimicrobial Ag/ZnO nanocomposites for functionalization of textile fabrics, Journal of Alloys and Compounds, 610 (2014) 244-249.
62. G. Nagaraju, Udayabhanu, Shivaraj, S.A. Prashanth, M. Shastri, K.V.Yathish, C. Anupama, D. Rangappa, Electrochemical heavy metal detection, photocatalytic, photoluminescence, biodiesel production and antibacterial activities of Ag–ZnO nanomaterial, Materials Research Bulletin, 94 (2017) 54-63.
63. Y. Wei, Y. B. Chong, H. Du, J. Kong, C. He, Loose Yarn of Ag-ZnO-PAN/ITO Hybrid Nanofibres: Preparation, Characterization and Antibacterial Evaluation, Materials & Design, 139 (2018) 153-161.
64. Phuong, N.-T., Rtimi S., Claudiane Ouellet Plamondon. Nanomaterials Based Coatings: Fundamentals and Applications; Elsevier: Amsterdam, The Netherlands, 2019. ISBN: 9780128158845.
65. Nguyen Tri, P.; Guinault, A.; Sollogoub, C. Élaboration et propriétés des composites polypropylène recyclé/fibres de bambou. Matér. Tech. 2012, 100, 413–423. [Google Scholar] [CrossRef][Green Version]
66. Azizi, S.; David, E.; Fréchette, M.F.; Nguyen-Tri, P.; Ouellet-Plamondon, C.M. Electrical and thermal conductivity of ethylene vinyl acetate composite with graphene and carbon black filler. Polym. Test. 2018, 72, 24–31.

67. Azizi, S.; David, E.; Fréchette, M.F.; Nguyen-Tri, P.; Ouellet-Plamondon, C.M. Electrical and thermal phenomena in low-density polyethylene/carbon black composites near the percolation threshold. J. Appl. Polym. Sci. 2018, 47043.
68. Boukehili, H.; Nguyen-Tri, P. Helium gas barrier and water absorption behavior of bamboo fiber reinforced recycled polypropylene. J. Reinf. Plast. Compos. 2012, 31, 1638–1651. [Google Scholar]
69. Nguyen Tri, P.; Gilbert, V. Non-isothermal Crystallization Kinetics of Short Bamboo Fiber-reinforced Recycled Polypropylene Composites. J. Reinf. Plast. Compos. 2010, 29, 2576–2591. [Google Scholar]
70. Nguyen Tri, P.; Sollogoub, C.; Guinault, A. Relationship between fiber chemical treatment and properties of recycled pp/bamboo fiber composites. J. Reinf. Plast. Compos. 2010, 29, 3244–3256. [Google Scholar]
71. Tri, P.N.; Rtimi, S.; Nguyen, T.A.; Vu, M.T. Physics, Electrochemistry, Photochemistry, and Photoelectrochemistry of Hybrid Nanoparticles. In Noble Metal-Metal Oxide Hybrid Nanoparticles; Woodhead Publishing: Sawston, UK, 2019; pp. 95–123.
72. Nguyen Tri, P.; Ouellet-Plamondon, C.; Rtimi, S.; Assadi, A.A.; Nguyen, T.A. Methods for Synthesis of Hybrid Nanoparticles. In Noble Metal-Metal Oxide Hybrid Nanoparticles; Woodhead Publishing: Sawston, UK, 2019; pp. 51–63.
73. Nguyen, T.V.; Nguyen Tri, P.; Nguyen, T.D.; El Aidani, R.; Trinh, V.T.; Decker, C. Accelerated degradation of water borne acrylic nanocomposites used in outdoor protective coatings. Polym. Degrad. Stabil. 2016, 128, 65–76.
74. Nguyen Tri, P.; Prud'homme, R.E. Crystallization and Segregation Behavior at the Submicrometer Scale of PCL/PEG Blends. Macromolecules 2018, 51, 7266–7273. [Google Scholar] [CrossRef]
75. Nguyen, T.P. Nanoscale analysis of the photodegradation of Polyester fibers by AFM-IR. J. Photochem. Photobiol. A Chem. 2018, 371, 196–204.
76. Tri, P.N.; Prud'homme, R.E. Nanoscale Lamellar Assembly and Segregation Mechanism of Poly(3-hydroxybutyrate)/Poly(ethylene glycol) Blends. Macromolecules 2018, 51, 181–188.
77. El Aidani, R.; Nguyen-Tri, P.; Malajati, Y.; Lara, J.; Vu-Khanh, T. Photochemical aging of an e-PTFE/NOMEX® membrane used in firefighter protective clothing. Polym. Degrad. Stabi. 2013, 98, 1300–1310.
78. Zeb, G.; Tri, P.N.; Palacin, S.; Le, X.T. Pulse potential deposition of thick polyvinylpyridine-like film on the surface of titanium nitride. RSC Adv. 2016, 6, 80825–80829.
79. Nguyen, T.V.; Le, X.H.; Dao, P.H.; Decker, C.; Nguyen-Tri, P. Stability of acrylic polyurethane coatings under accelerated aging tests and natural outdoor exposure: The critical role of the used photo-stabilizers. Prog. Org. Coat. 2018, 124, 137–146.